Available online at www.sciencedirect.com
ScienceDirect
Acta Materialia 54 (2006) 5393–5399
Acta MATERIALIA
www.actamat-journals.com

Converting polycrystals into single crystals – Selective grain growth by high-energy ion bombardment

Sven Olliges [a], Patric Gruber [b], Anita Bardill [a], Daniel Ehrler [a], Heinz Dieter Carstanjen [c], Ralph Spolenak [a,*]

[a] *Laboratory for Nanometallurgy, Department of Materials, ETH Zurich, Wolfgang-Pauli-Strasse 10, 8093 Zurich, Switzerland*
[b] *Universität Stuttgart, Institut für Metallkunde, Heisenbergstrasse 3, 70569 Stuttgart, Germany*
[c] *Max Planck Institute for Metals Research, Heisenbergstrasse 3, 70569 Stuttgart, Germany*

Received 24 March 2006; received in revised form 6 July 2006; accepted 7 July 2006
Available online 27 September 2006

Abstract

Common failure mechanisms in microelectronics such as electromigration, creep and fatigue can be positively influenced by microstructure optimization. In this paper a new mechanism of microstructure optimization in thin metal films is proposed. Post-deposition ion bombardment can produce an in-plane texture in originally highly fiber textured thin metal films by a selective grain growth process. In extreme cases the in-plane texture becomes as sharp as the out-of-plane fiber texture. A subset of grains oriented for ion channeling was found to grow significantly at the expense of the remaining grain fraction. We studied the selective grain growth as a function of ion species (N^+, Ne^+, Ar^+), ion energy (1–3.5 MeV) and target temperature (liquid nitrogen to 400 °C). In a textured thin film the degree of preferred in-plane orientation can be strongly influenced by ion bombardment, and therefore this technique has the potential to become a powerful tool for the enhancement of reliability in micro- and nanosystems.

Keywords: Ion-beam processing; Electron backscattering diffraction; Thin films; Crystal growth

1. Introduction

The texture of thin metal films can be controlled by ion bombardment assisted deposition [1–3]. Dong and Srolovitz [1,2] report in their theoretical work two main effects that influence film texture during deposition: (a) the anisotropy of the sputter rate, and (b) the anisotropic generation of defects due to ion bombardment; the latter effect is the stronger. Due to anisotropic defect generation, less damaged grains grow at the expense of strongly damaged grains. Minimization of the free volume energy is the driving force.

Changes to thin film texture caused by post-deposition ion bombardment were observed by Spolenak et al. [4,5] in a focused ion beam (FIB) microscope. They observed selective ion-induced grain growth in near-surface regions of thin gold and copper films by 30 keV Ga^+ bombardment, where the grains showing channeling grow at the expense of the grains showing no channeling. Since the cross-section for defect generation is reduced under channeling when compared to non-channeling conditions, the results are qualitatively consistent with the simulations of Dong and Srolovitz [1,2] and the experimental observations of Park et al. [3], respectively.

To date, no selective grain growth by ion bombardment in the 1.0–4.0 MeV range has been observed. In the present work, experiments with a variety of ion species, ion bombardment temperatures (T_{irr}) and ion energies were performed to control the texture in existing thin gold films. Because of the high ion energy the effect was observable also in non-near-surface regions in the 500–1000 nm depth range. Since the influence of ion bombardment on the

* Corresponding author.
E-mail address: ralph.spolenak@mat.ethz.ch (R. Spolenak).

1359-6454/$30.00
doi:10.1016/j.actamat.2006.07.005

average grain size is well known [6,7], in the present paper we focus on the development of in-plane textures.

2. Experimental

Polycrystalline gold thin films were deposited under ultrahigh vacuum conditions (10^{-9} mbar) on a silicon substrate coated with 50 nm SiO_2 and 50 nm Si_3N_4 by magnetron sputtering at room temperature (RT). Before deposition, the substrate surface was cleaned by 1 keV Ar^+ bombardment for 1 min. The thin gold films show a strong (1 1 1) fiber texture parallel to the surface normal. The grains have a mean diameter of approximately 80 nm and a columnar structure; the thicknesses of the films are 500 and 1000 nm.

The [1 1 0] axes are the main channeling axes in the face-centered cubic (fcc) lattice. Since one [1 1 1] axis of any grain is parallel to the surface normal, ion channeling along [1 1 0] corresponds to an incident angle of 35.24° to the surface normal (given by the angle between the [1 1 1] and [1 1 0] directions, Fig. 1). Small variations in the incident angle are permitted; their size should just be smaller than the critical angle for axial ion channeling in crystals as derived by Lindhard [8]

$$\psi_c = \sqrt{\frac{2Z_1Z_2e^2}{d \cdot E}}, \tag{1}$$

where $Z_{1,2}$ are the atomic numbers of the incident ions and target atoms, respectively, d the distance of adjacent atoms in an atomic chain, E the ion energy in eV and $e^2 = 14.4$ eVÅ the square of the elementary charge. For 1 MeV N^+, as used here in one of the irradiation experiments, the critical angle for the [1 1 0] main channel axis in gold is calculated to be 4.3°.

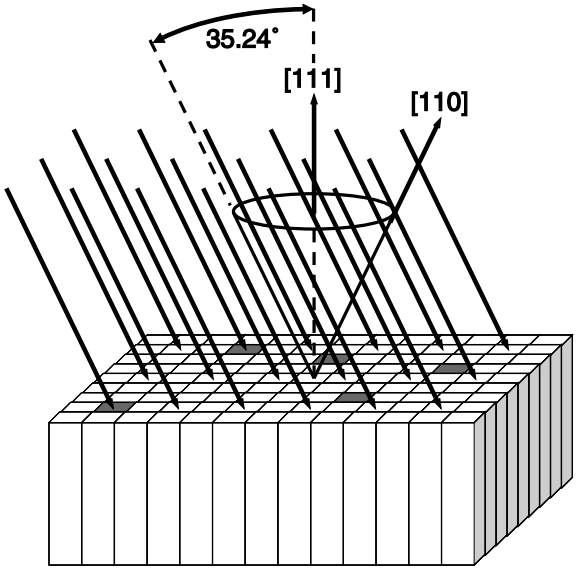

Fig. 1. Schematic drawing of the experimental situation in a (1 1 1) textured film. One [1 1 1] axis of any grain is parallel to the surface normal while the other [1 1 1] axes are distributed randomly due to one degree of freedom with respect to the surface normal. The [1 1 0] axes form a cone with an angle of 35.24° to the surface normal.

The thin films were irradiated with 1.0–3.5 MeV N^+, Ne^+ and Ar^+ ions with the ion beam direction at an angle of 35.24° to the surface normal using the 6.5 MV Pelletron accelerator of the Max Planck Institute (MPI) for Metals Research in Stuttgart. The ion fluences were in the region of 10^{17} ions/cm^2 and the target currents in the 10–100 nA range, depending on the ion species. The temperature during ion irradiation was kept at either liquid nitrogen (LN_2, approximately −180 °C) temperature, RT or 400 °C, respectively. After ion bombardment, the beam spots on the target were measured using a dark-field optical microscope to calculate the respective ion fluence from the total ion charge collected on the target. Normalized pole figures, obtained by electron backscatter diffraction (EBSD) using an HKL Channel 5 EBSD detector in a LEO 1530 VP scanning electron microscope at the MPI for Metals Research, Stuttgart, display the thin film texture before and after ion bombardment.

The area of the beam spot exceeded the grain size by eight orders of magnitudes. Thus, only a few irradiated grains showed channeling while the rest showed non-channeling behavior. For a polycrystalline thin film with (1 1 1) texture normal to the surface, but otherwise random orientation, the percentage of grains showing channeling is given by

$$p = \frac{\psi_c \cdot n}{4 \cdot \sin\alpha} = \frac{A_i}{A_0} \tag{2}$$

for $\alpha > \psi_c$, where ψ_c is the critical angle of the investigated system, n the symmetry group C_n of the channeling system with respect to the surface normal, and α the angle between the beam and the surface normal. In the present case of the [1 1 0] direction, $n = 3$, $\alpha = 35.24°$ and $\psi_c = \psi_c([1\,1\,0], E, Z_1, Z_2)$. This expression is equivalent to the normalized subset A_i showing channeling of an area A_0. In the current investigations the critical angles are in the regime of 4° which corresponds to approximately 9% of the grains (or area) showing channeling.

In comparison to non-channeling, the interaction between ions and lattice-atoms is strongly reduced due to the lattice-steering effect during ion channeling [9], which results in a non-uniform generation of defects in the thin film. According to previous theoretical and experimental investigations [1,2,4], we expect changes in the in-plane texture due to ion-induced selective grain growth, where the fully rotational degree of freedom with respect to the [1 1 1] axis (parallel to the surface normal) is reduced to a cone of the size of the critical angle ψ_c along the direction of the incident ion beam.

3. Results

Fig. 2(a) shows the initial pole figure of an untreated thin film (1000 nm thick). It exhibits a sharp peak in the centre of the {1 1 1} pole figure corresponding to the

(1 1 1) texture of the film parallel to the surface and a ring corresponding to randomly distributed further {1 1 1} planes which are tilted by an angle of $\psi = 70.54°$ to the surface normal.

In comparison to the as-deposited sample, the film irradiated with 3.5 MeV Ne^+ at RT to a fluence of 3.2×10^{17} ions/cm^2 (Fig. 2(b)) shows a superposition of a random (1 1 1) texture and a C_3 symmetry around the [1 1 1] axis: the (1 1 1) texture persists as indicated by the sharp peak in the centre of the {1 1 1} pole figure, while the previously random in-plane orientation has changed to a favored in-plane orientation. Since the mean grain size has increased from 80 nm to approximately 1000 nm, we assume that the development of the favored in-plane orientation is due to selective ion-induced grain growth.

Irradiation of 1000 nm thin films with 1 MeV N^+ ions and 3.5 MeV N^+ ions, but the same fluence of $\sim 4 \times 10^{17}$ ions/cm^2 at RT, shows the influence of the ion energy on the ion-induced selective grain growth (Fig. 3). At 3.5 MeV only a weak C_3 symmetry is observed in comparison to the irradiation with ions of lower energy where the random signal is reduced and a clear C_3 symmetry obtained.

In order to investigate the temperature dependence of this selective growth process 500 nm Au films were irradiated with 1 MeV N^+ ions at high temperature (400 °C) and at LN_2 temperature with a fluence of 10^{17} ions/cm^2 (Fig. 4). At 400 °C a weak C_3 symmetry with a wide angular distribution of the orientation of the grains is observed (Fig. 4(a)), while at LN_2 temperature a superposition of

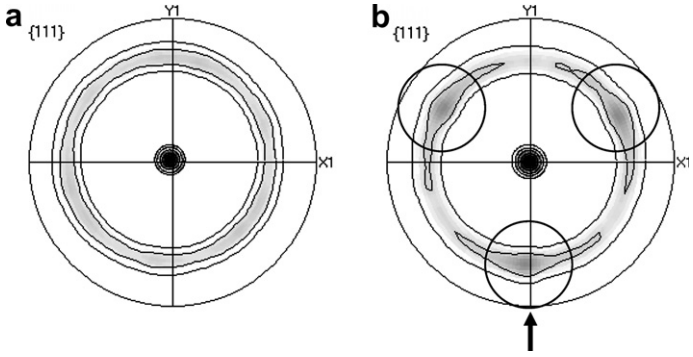

Fig. 2. EBSD pole figures of (a) an untreated Au sample and (b) an Au sample which was irradiated with 3.5 MeV Ne^+ to a fluence of 3.2×10^{17} ions/cm^2 at RT. The arrow shows the projection of the ion beam. Sample thickness 1000 nm.

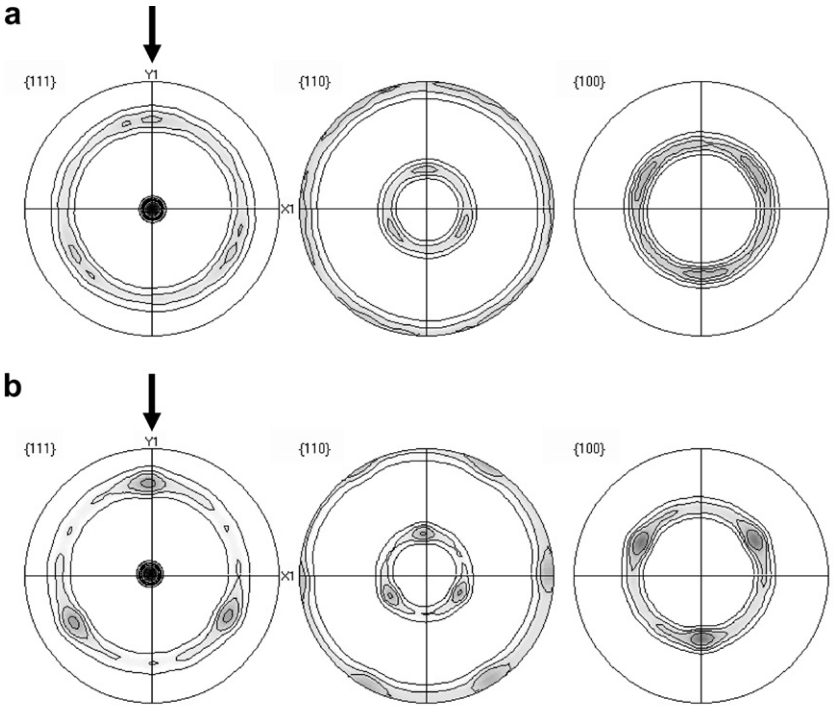

Fig. 3. Pole figures of Au samples irradiated at RT with (a) 3.5 MeV N^+ and (b) 1 MeV N^+ ions to a fluence of $\sim 4 \times 10^{17}$ ions/cm^2. The arrows show the corresponding projection of the ion beam. Sample thickness 1000 nm.

two C_3 symmetries with sharp peaks is obtained (Fig. 4(b)). The superposition of two C_3 symmetries is due to two "active" channel axes. The additionally observed peak, rotated by an angle of ~80°, corresponds to an active [3 2 0] channel axis. The widths (FWHM) of the peaks are 6° for [1 1 0] and 4° for [3 2 0] which are slightly smaller than the by a geometrical factor corrected apex angles (opening angle of the cone) of the system (10° for [1 1 0] and 5° for [3 2 0]). The obtained C_3 symmetry at LN_2 temperature is considerably sharper than at 400 °C.

In order to check the dependence on ion mass, a 500 nm Au film was irradiated with 2.5 MeV Ar^+ ions and a fluence of 1.5×10^{17} ions/cm^2 at LN_2 temperature. The pole figure (Fig. 5) shows very narrow peaks which are in good agreement with those of a single crystal. In the in-plane grain map, 94.3% of the identifiable scanned surface is aligned in the same direction. The angular distribution of the peaks is approximately 5° (FWHM), which is much smaller than the corrected apex angle of approximately 10.5° for the system. Only a few single grains are observed in the grain map, and the grains oriented in the same direction are affiliated to domains. In comparison to the findings of Spolenak et al. [4,5], the effect occurs throughout the entire film thickness as can be seen in the FIB picture of the EBSD-scanned area (Fig. 6).

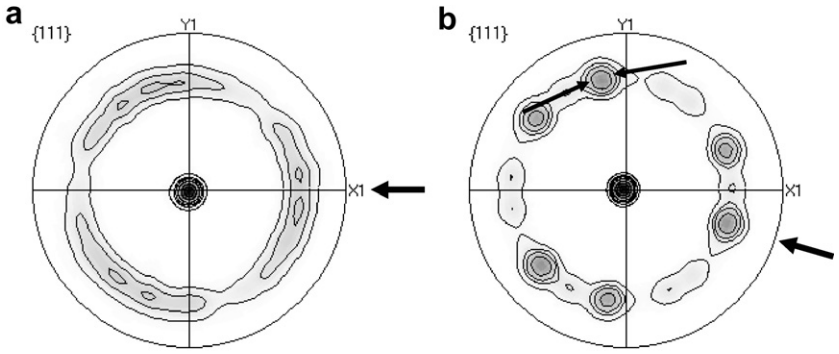

Fig. 4. EBSD pole figures of 500 nm Au irradiated with 1 MeV N^+ to a fluence of 10^{17} ions/cm^2 at (a) 400 °C and (b) LN_2 temperature. The arrows show the corresponding projection of the ion beam.

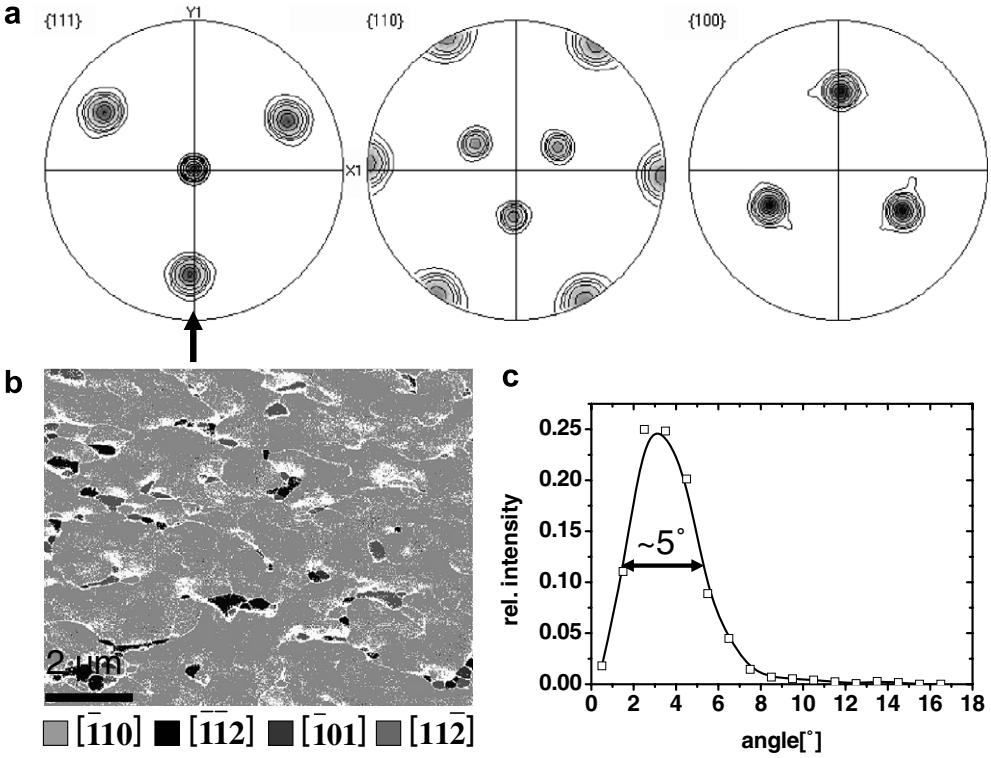

Fig. 5. (a) EBSD pole figures of 500 nm Au irradiated with 2.5 MeV Ar^+ and 1.5×10^{17} ions/cm^2 at LN_2 temperature (the arrow shows the projection of the ion beam), (b) corresponding grain map and (c) corresponding angle distribution of the [$\bar{1}$10] direction. The fraction of the [11$\bar{2}$], [$\bar{1}\bar{1}$2] and [$\bar{1}$01] directions are negligible and not shown. The white areas are unindexed parts of the surface.

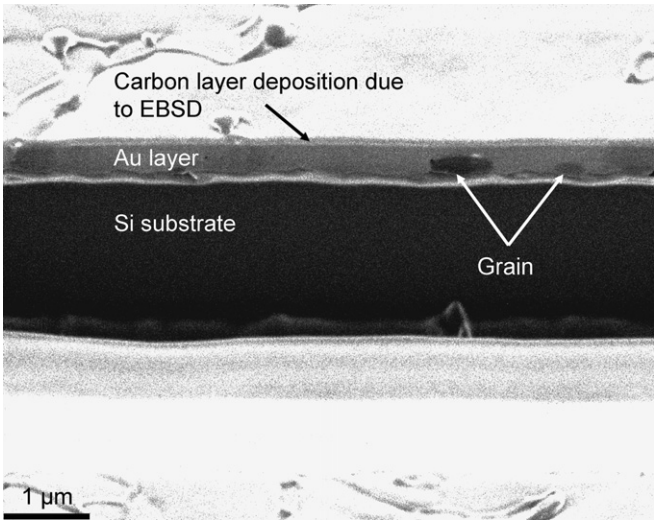

Fig. 6. FIB image (tilt angle: 45°, ions: 30 keV Ga^+, target current: 5 pA, secondary electron mode) of a cross-section of the 500 nm Au thin film on Si substrate irradiated with 2.5 MeV Ar^+ and a fluence of 1.5×10^{17} ions/cm^2 at LN_2 temperature. The FIB section was made on the area used for EBSD analysis (cf. Fig. 5). The large dark part corresponds to the Si substrate, the intermediate gray layer shows the Au layer and the bright thin coverage on the top of the gold film is due to carbon deposition during EBSD measurements. There are still some small embeddings with different contrast in the Au layer but in comparison to previous studies [4,5], the selective ion-induced grain growth occurs throughout the entire film thickness in the majority of the grains (compare Fig. 6 in [4]).

4. Discussion

We assume a model with columnar grains (length t = film thickness) with quadratic base of an initial edge length d_i. A fraction p (see Eq. (2)) of these grains may have the proper orientation for channeling. A limitation for ion-induced grain growth is set by the film thickness: if the grains have an initial edge length d_i of the size of the film thickness t, the grain growth is strongly inhibited as reported by Li et al. [7] and Mullins [10]. For growth to occur, the initial edge length of the grains, d_i, must be significantly smaller than the length t of the columnar grains. In order to obtain full texture control, the grains must exhibit a minimum initial aspect ratio a (film thickness t divided by the initial edge length $d_i^{\min}$) which is given by

$$a_{\min} = \frac{t}{d_i^{\min}} = \frac{1}{\sqrt{p_i}}, \tag{3}$$

where p_i is the initial percentage of grains showing channeling. If ion-induced selective grain growth is the only grain growth mechanism, full texture control in gold is possible at an aspect ratio of $a > 3.3$ for channeling of 1 MeV N^+ along the [1 1 0] main channeling axis (see Eq. (2) for $n = 3$). If the aspect ratio of the grains has decreased by a factor $f > 1$ from a to $\hat{a} = a/f$ (due to grain growth), the percentage $\hat{p}$ of the aligned area is given by

$$\hat{p} = \frac{\widehat{A}}{A_0} = p_i \cdot f^2, \tag{4}$$

where p_i is the initial percentage of the area showing channeling, $\widehat{A}$ the aligned and A_0 the total area. For full texture control the percentage $\hat{p}$ is equal to 1, which yields $f = \sqrt{1/p_i}$ for the maximum possible growth factor in the frame of the present model. If there are different (not equivalent) axes showing channeling, the overall percentage of the aligned area is given by the superposition of the respective contributions

$$\hat{p}_{\text{tot}} = \sum_j \hat{p}_j. \tag{5}$$

The grain size in the 3.5 MeV Ne^+ experiment has changed by $f \approx 11$ which is larger than the calculated value of 4 (see Eqs. (1)–(3)) for full texture control. Since the texture has not changed completely from random to single crystalline orientation (cf. Fig. 2) we conclude that both selective as well as normal non-directional grain growth have occurred simultaneously. Hence we have to distinguish between these two contributions to ion-induced grain growth.

The energy dependence (alignment of the surface after ion irradiation: ~31% for 3.5 MeV N^+ and ~44% for 1 MeV N^+) evident from the irradiations at 3.5 MeV N^+ and 1.0 MeV N^+ is most probably due to the energy dependence of the generation of defects in the thin film which is governed by the nuclear stopping power. It is – in the present energy range – proportional to [11]

$$\left.\frac{dE}{dx}\right|_n \propto \frac{\ln(E)}{2E}. \tag{6}$$

Therefore fewer defects are deposited in the thin film than at lower ion energy. From SRIM calculations [12], a theoretical depth-dependent defect concentration according to

$$\rho(x) = \text{fluence} \cdot \frac{\text{number of defects}\,(x)}{\text{ion} \cdot \text{length}}, \tag{7}$$

can be obtained, where the "number of defects/(ion · length)" is obtained by the SRIM code as a function of depth x in the same sample. The units of ρ are number of defects/volume, which corresponds to a defect density. ρ actually represents the produced concentration of vacancies, but does not take into account losses by, for example, recombination with interstitials. For 1.0 MeV N^+, approximately four times the defects of 3.5 MeV N^+ are generated within the top 500 nm of the thin film according to SRIM. From this we conclude that ion-induced selective grain growth depends on the overall generation of defects per volume instead of the fluence. It should also be noted that the critical angle for ion channeling and therefore the required initial minimum aspect ratio depend on the ion energy as evident from Eqs. (1)–(3).

A key observation is that the selective grain growth process is more pronounced at LN_2 temperature than at higher temperatures. For 1 MeV N^+ bombardment at LN_2 temperature (10^{17} ions/cm^2) the average grain diameter has increased by a factor of 2.9 which is close to the calculated value of 2.6 for full texture control.

The superposition of two C_3 symmetries seen in Fig. 4, which has not been observed before, is due to small sample misalignment. At these energies the cone of the [1 1 0] main channel direction and the cone of the additional [3 2 0] channeling axis show an overlap that can result in ion channeling in both directions and in selective ion-induced grain growth in two favored directions. Nevertheless, the pole figure shows the superposition of two sharp C_3 symmetries in addition to a low random signal.

The well-oriented grains observed in most of the pole figures are affiliated to continuous domains only after 2.5 MeV Ar^+ bombardment. The rate of defect generation in this case is considerably higher than with N^+ and Ne^+ ions which is due to (a) the increased nuclear stopping power caused by the larger ion nuclear charge and mass of the Ar^+ ions and, therefore a much higher defect production rate, and (b) possibly due to a higher target current (100 nA for 2.5 MeV Ar^+, 10–15 nA for 1 MeV N^+ and 40–45 nA for 3.5 MeV Ne^+). In comparison to 1 MeV N^+ and 3.5 MeV Ne^+, the defect generation rate for 2.5 MeV Ar^+ is higher by factors of 35 and 15, respectively. Hence, we conclude that the amount of damage and possibly also the damage rate have great influence on the ion-induced selective grain growth.

Our results are consistent with theoretical and experimental investigations of Carter [12], Dong and Srolovitz [1,2], Park et al. [3] and Spolenak et al. [4]. However, in the bimolecular model for grain boundary motion proposed by Atwater et al. [6], the boundary shifts into the less damaged grain, which is contrary to our experimental observations. Hence, as mentioned earlier, we have to distinguish between normal, non-directional and selective grain growth processes.

The non-directional grain growth can be described by the established models for grain growth driven by grain boundary energy minimization [6]. In the following, we propose a model according to Zaiser et al. [13] for ion-induced transformation of graphite into diamond that could account for the observed effects. We consider a grain boundary between a grain oriented favorably for channeling and a grain oriented unfavorably for channeling. The channeling effect causes an inhomogeneous generation of defects, i.e. many defects in the grain not permitting channeling and by about one order of magnitude less in grains permitting channeling. The atoms in the grain boundary oscillate with Debye's frequency ω_D about their current positions. During the oscillation, desorption from one side and reorganization of the atoms on the corresponding opposite side of the grain boundary take place. Desorption from the highly damaged side and reorganization on the opposite, less-damaged side releases energy, since the free volume energy F_{ges} is higher in the grain with defects. The observed temperature dependence (irradiation at LN_2 temperature, RT and 400 °C) is most probably due to the immobility of the vacancies at low temperatures [14,15] where only interstitials can migrate to the grain boundaries resulting in the observed selective grain growth. At 400 °C, i.e. well above stage III temperatures, vacancies also become mobile, and therefore strongly increased annihilation of vacancies and interstitials in the matrix as well as at the grain boundary occurs, resulting in less-pronounced directional grain growth.

Finally, the sign of the boundary shift depends on the gradient in chemical potential $\Delta\mu$ given by [4]

$$\frac{dr}{dt} = M_{eff}(\Delta\mu_{GB} + \Delta\mu_{defects}), \tag{8}$$

where $\Delta\mu_{GB}$ is the difference in chemical potential as determined by the minimization of grain boundary volume, $\Delta\mu_{defects}$ the difference in chemical potential due to differences in volume defect density, M_{eff} the effective grain boundary mobility and r the grain radius. At high temperatures (e.g. 400 °C) the annihilation of vacancies and interstitials occurs at a high rate and thus the defect gradient term $\Delta\mu_{defects}$ is reduced and normal grain growth dominates (cf. Fig. 4). At low temperatures (e.g. −180 °C) vacancies are immobilized and $\Delta\mu_{defects}$ consequently becomes dominant. Grain growth of grains oriented for channeling is strongly enhanced at these temperatures. However, the proposed model for selective ion-induced grain growth is speculative since to date no experimental data for selective ion-induced grain growth kinetics are available.

5. Summary and outlook

Ion bombardment under channeling condition results in ion-induced selective grain growth in thin gold films. We have shown that the ion energy, the ion species and particularly the temperature during irradiation influence the selective grain growth process. Surprisingly, the effect is much more pronounced for ion bombardment at LN_2 temperature than at RT and 400 °C, which probably is due to the increased annihilation of vacancies and interstitials at elevated temperatures. For irradiation with Ar^+ ions at LN_2 temperature a nearly complete single-crystalline microstructure is obtained. Local differences in free volume energy ΔF due to the anisotropic generation of defects during ion irradiation (ion channeling effect) are deemed to be the driving forces for this process.

Further experiments will be performed to investigate the applicability in micro- and nanosystems, e.g. the extension to other common materials like copper. In addition key experiments are envisioned that investigate the kinetics of the growth process to formulate a quantitative model for selective ion-induced grain growth.

Acknowledgements

We gratefully acknowledge the MPI's Thin Film Laboratory, namely Gerhard Adam and Ilse Lakemeyer, for sample fabrication, the MPI's pelletron staff, namely Michael Bechtel and Saroj Prashad Dash, for their support during beamtimes, Birgit Heiland (MPI for Metals

Research, Stuttgart) for FIB microscope operation and Christian Solenthaler (LNM, ETH Zurich) for helpful and fruitful discussions.

References

[1] Dong L, Srolovitz DJ. Appl Phys Lett 1999;75:4.
[2] Dong L, Srolovitz DJ. J Appl Phys 1998;84:9.
[3] Park SJ, Norton DP, Selvamanickam V. Appl Phys Lett 2005;87:031907.
[4] Spolenak R, Sauter L, Eberl C. Scr Mater 2005;53:1291.
[5] Spolenak R, Pérez Prado MT. Scr Mater 2006;55:103.
[6] Atwater HA, Thompson CV, Smith HI. J Appl Phys 1988;64:5.
[7] Li J, Liu JC, Mayer JW. Nucl Instr Meth Phys Res B 1989;36:306.
[8] Lindhard JK. Dan Vidensk Selsk Mat Fys Medd 1965;34:14.
[9] Gemmell DS. Rev Mod Phys 1974;46:1.
[10] Mullins WW. Acta Metall 1958;6:414.
[11] Ziegler JF, Biersack JP, Littmark U. In: The stopping and ranges of ions in solids. New York: Pergamon Press; 1985.
[12] Carter G. Phys Rev B 2000;62:12.
[13] Zaiser M, Lyutovich Y, Banhart F. Phys Rev B 2000;62:5.
[14] Balluffi RW. J Nucl Mater 1978;69–70:240.
[15] Young FW. J Nucl Mater 1978;69–70:310.